Measurements of Heat and Moisture Fluxes from the Western Tropical Pacific Ocean

E.F. BRADLEY[1], P.A. COPPIN[1] and J.S. GODFREY[2]

[1] *CSIRO Centre for Environ. Mechanics, GPO Box 821, Canberra, ACT 2601 - Australia*

[2] *CSIRO Division of Oceanography, GPO Box 1538, Hobart, Tas. 7001 - Australia*

ABSTRACT

Micrometeorological measurements, including direct eddy-correlation heat and moisture fluxes, have been made under light wind conditions in the western equatorial Pacific. The sea surface "cool skin" of about 0.5°C was observed; air-sea temperature differences were 1-1.5°C larger than longterm averages from merchant-ship data. Bulk transfer coefficients for both fluxes increased markedly as wind speed fell below 4 m/s, in excellent agreement with the predictions of Liu et al. (1979). Dissipation estimates of the fluxes are about half the covariance measurements below 4 m/s. Observations of the individual components of radiation suggest that commonly used empirical formulations overestimate both long- and shortwave in this region by 15-20 W/m^2. application of all possible corrections would reduce Reed's (1985) estimate of net heat flux into the ocean by some 80 W/m^2 to around only 20 W/m^2 in this region of the Pacific.

1. INTRODUCTION

Thermodynamic interactions between atmosphere and ocean in the equatorial western Pacific play a dominant role in determining global weather patterns including, as an extreme example, the well-documented El Nino - Southern Oscillation (ENSO) phenomenon. One well-known precursor of ENSO is the sea surface temperature (SST) anomaly in the tropical Pacific, and eastward displacement of the so-called "warm pool" normally situated just northeast of New Guinea. Clearly, such changes to SST must result from variations in some or all of various components of the near-surface heat balance of the ocean; i.e. advective or diffusive transport within the ocean body itself and ocean-atmosphere coupling.

A much better understanding of the physics and dynamics of these transport processes is required if SST is to be properly simulated in models of the coupled ocean-atmosphere system. Several authors (e.g. Ramage 1984, Schlesinger and Mitchell 1987) agree that, in the context of climate change research, an additional energy input of only 10 W/m^2 to the ocean and troposphere would be very significant. Yet, as Godfrey and Lindstrom (1989) point out, uncertainty of the order of 80 W/m^2 is apparent in current climatological estimates of the heat budget of the surface mixed layer of this region. They estimated that only 5-10 W/m^2 could be mixed downwards through the surface isothermal layer; other authors (Enfield 1986, Niiler and Stevenson 1982) found that horizontal advection in this region is also only 5-10 W/m^2. This leads to an estimated net capacity for the ocean to carry heat away from the surface of 10-20 W/m^2. This is smaller than four recent estimates of the long-term mean heat flux into this region (Weare et al. 1981, Esbensen and Kushnir 1981, Reed 1985, Hsiung 1985), which range between 25 and 80 W/m^2.

Either there are horizontal transport processes unaccounted for by earlier authors, such as the eddies seen in the eastern Pacific (Legeckis et al. 1983); or some unknown and quite large source of turbulent kinetic energy must exist to mix this heat flux downwards; or the heat flux estimates must all be too large.

The exchange of energy between the ocean and the atmosphere is given by the heat budget:

$$N = S - L - H - E \tag{1}$$

where the net heat input to the ocean, N, results from the absorption of solar radiation, S, less amounts lost to the atmosphere through net longwave radiative transfer, L, sensible heat flux, H, and latent heat flux, E. Annual values of the quantities on the right-hand side of the equation have been calculated for the tropical Pacific region by the authors mentioned above using ship-of-opportunity observations. S is dominated by cloud cover; L by sea surface temperature, atmospheric water vapour content and cloudiness; and H and E by turbulent transfer processes which depend on wind speed, sea state and air-sea temperature differences. Sensible and latent heat fluxes are usually estimated from bulk transfer relationships:

$$H = \rho C_p \bar{U} C_H (T_s - T_a) \tag{2}$$

$$E = \rho L_E \overline{U} C_E (q_s - q_a) \quad (3)$$

where ρ and C_p are the density and specific heat of air, L_E is latent heat of vaporisation, $\overline{U}$ the mean wind speed and T and q the temperature and specific humidity in air at some specified level and at the water surface according to the subscripts. C_H and C_E are empirically defined bulk transfer coefficients.

Individual estimates of the fluxes at a particular location vary considerably, partly a result of the different formulations used to convert the data; S, for example, over the range 160–225 W/m^2, L from 60–120 W/m^2 . Blanc (1985) reviews ten variations on equations (2) and (3), illustrating particularly the wide range of transfer coefficients C_H and C_E in common use. There are also, we believe, systematic biases resulting from the rather special weather conditions prevailing in the western equatorial Pacific which may preclude the use of parameters determined for other parts of the globe. Frequent convective storms, localised and with high cumulus towers, make any objective, regional specification of cloud cover almost impossible. Frequent rainstorms provide a source of energy transfer not accounted for in the above heat budget. A further measure of uncertainty arises from the high humidity levels and light winds which are a feature of the region.

Between April 23 and May 25 1988, oceanographic measurements were made from R/V "Franklin", along the track shown in Figure 1, in the western equatorial Pacific. The primary purpose of the cruise was to make hydrographic and ocean turbulence measurements as a continuation of the WEPOCS cruises (Lindstrom et al. 1987). However, a secondary purpose was to examine some aspects of the above heat budget discrepancy; there were four main objectives:

* to attempt direct eddy-correlation measurements of heat and moisture fluxes. This is not usually possible because of ship motion, so that indirect methods of flux measurement are used (bulk, profile, dissipation), all of which are believed to fail in light winds;
* to define bulk transfer coefficients for these very low wind conditions. Models predict a significant increase with approach to the free convection regime, but this has never been tested by experiment;
* to make accurate measurements of the sea–air temperature gradients and look for the "cool skin" effect, i.e. evaporative cooling of the actual water interface relative to the bulk temperature;
* to measure all the terms in the radiation budget.

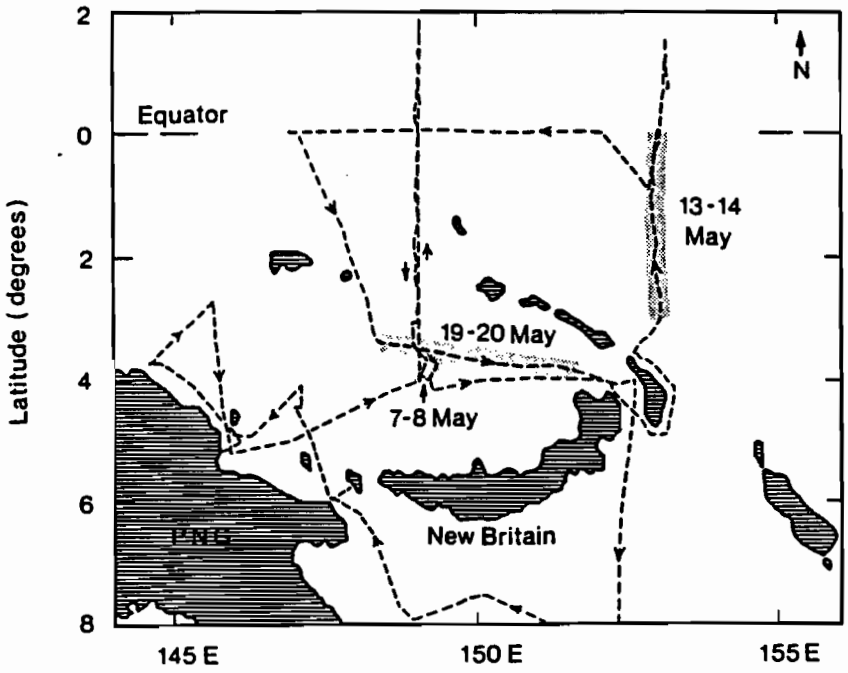

Figure 1. Cruise track of R/V "Franklin". Hatched sections show meteorological observation periods.

2. INSTRUMENTATION

The general layout of the vessel and instruments is shown in Figure 2. R/V "Franklin" is a Voluntary Observing Ship for WMO and makes the usual routine meteorological observations: wind speed and direction, engineroom thermograph temperature and wet and dry bulb air temperature at 6 h intervals. The engineroom intake is about 2 m below the surface and 13 m aft of the bow; temperature is measured about 1 s after water enters the ship. The air thermometers are located in a Stevenson screen above the bridge, and the anemometer atop the main mast.

Other meteorological equipment was mounted at the end of a retractable boom, 10 m forward of the bow to minimise disturbance to the air by the ship. The boom carried a vertical section, as shown in Figure 2, extending from about 3 m to 10 m above the sea surface. Cup anemometers and aspirated psychrometers were mounted at upper, middle (6 m) amd lower levels to obtain gradients. A 3-dimensional sonic anemometer (Coppin and Taylor 1983) and a Lyman-α humidiometer were also mounted at the 6 m level. Three orthogonal accelerometers were mounted on the boom about 1 m aft of the sonic anemometer, and pitch and roll sensors located near the ship's centre of gravity.

Three radiometers were installed: an Eppley pyranometer and a pyrgeometer at the top of the main mast and a net radiometer at the end of the boom. In addition, an infrared radiometer (kindly provided by Dr. Ian Barton) was mounted above the bridge and aimed at the sea surface, clear of the ship's wake. This radiometer has a bandpass of 1 micron centred on the 11 micron band similar to channel 4 of the AVHRR instrument.

Signals from the fast-response instruments (the sonic, Lyman-α and accelerometers) were recorded at 20 Hz sampling rate on digital computer tape. Time series were recorded continuously to fill a tape (about 5 h) and subsequently broken up into a sequence of 15 min runs. The other 'slow' sensors were sampled at 5 s intervals, and 15 min averages recorded on a data logger.

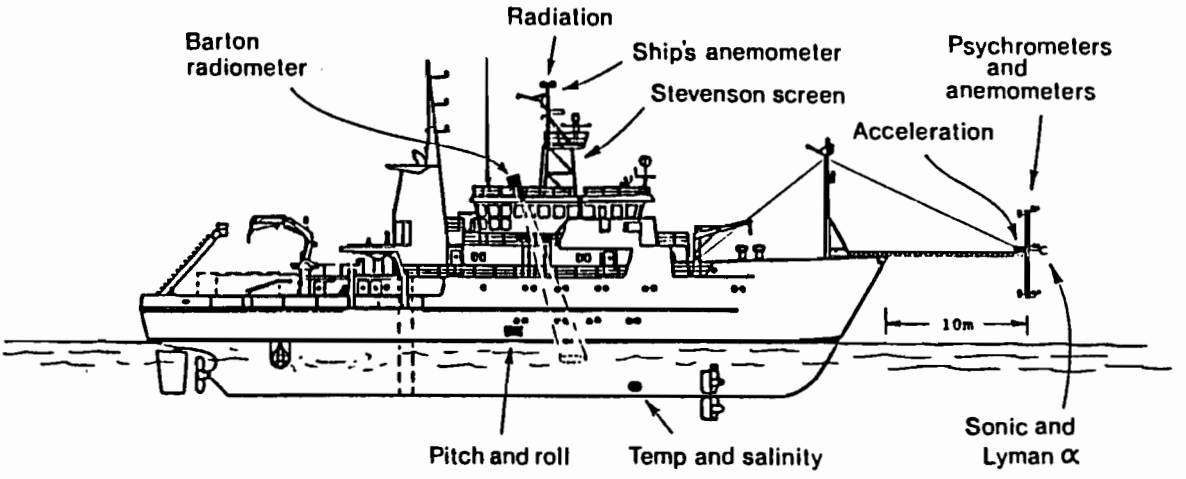

Figure 2. R/V "Franklin", (55 m 1200 t) and instrument locations.

3. OBSERVATION CONDITIONS

Data from the radiometers, cup anemometers and psychrometers were recorded continuously whenever possible throughout the cruise. During infrequent occasions of strong winds or heavy swell, when the bottom of the vertical boom section was in danger of dipping into the water, the boom was retracted to a position about 3 m forward of the bow. The sonic, Lyman-α and Barton radiometer were mounted only when conditions were favourable for eddy-flux measurement i.e. light wind, smooth sea and no rain. This occurred principally during three 24 h periods; two of these were in the Bismarck Sea with the ship's track determined by us; the third was during a northerly run from New Ireland to the equator. They are shown hatched in Figure 1.

The motion sensors were installed to enable ship motion to be removed from the wind signal. In the event, the pitch and roll sensors were inadequate so that correlations between fluctuating wind components, needed for stress and drag coefficient measurements, have not been possible. However, the scalar correlations are much less sensitive so that, with the almost imperceptible ship motion which occurred during our three observation periods (less than 1° pitch and 2° roll), covariance heat and moisture flux measurements were successful. Examples of spectra measured with a swell running, Figure 3, illustrates the ship's 10 s roll as a prominant peak in the vertical velocity spectrum. The humidity spectrum is clean, excepting for high frequency noise caused by the ship's engine vibration, and the cospectrum contains a notch at the roll frequency equivalent, however, to only 8% loss of moisture flux. In contrast, Figure 4 shows typical spectra from periods in which ship motion is imperceptible.

Because of the quiet sea conditions, also, the usual salt contamination problems created by spray were not encountered.

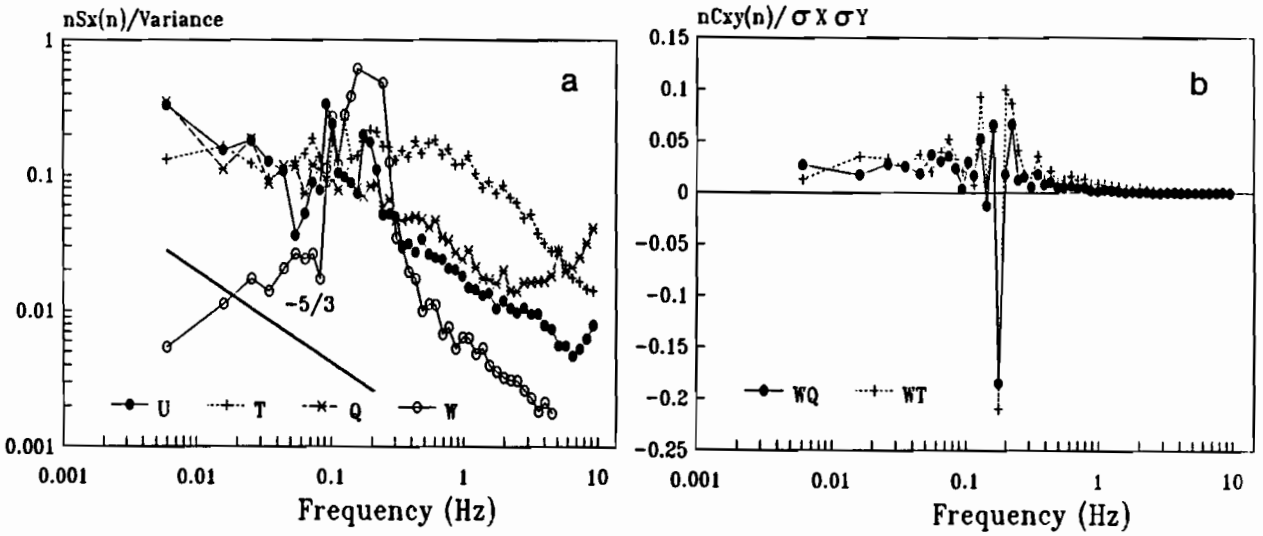

Fig 3. Normalized spectra (a) and Co-spectra (b) for a period of high ship motion.

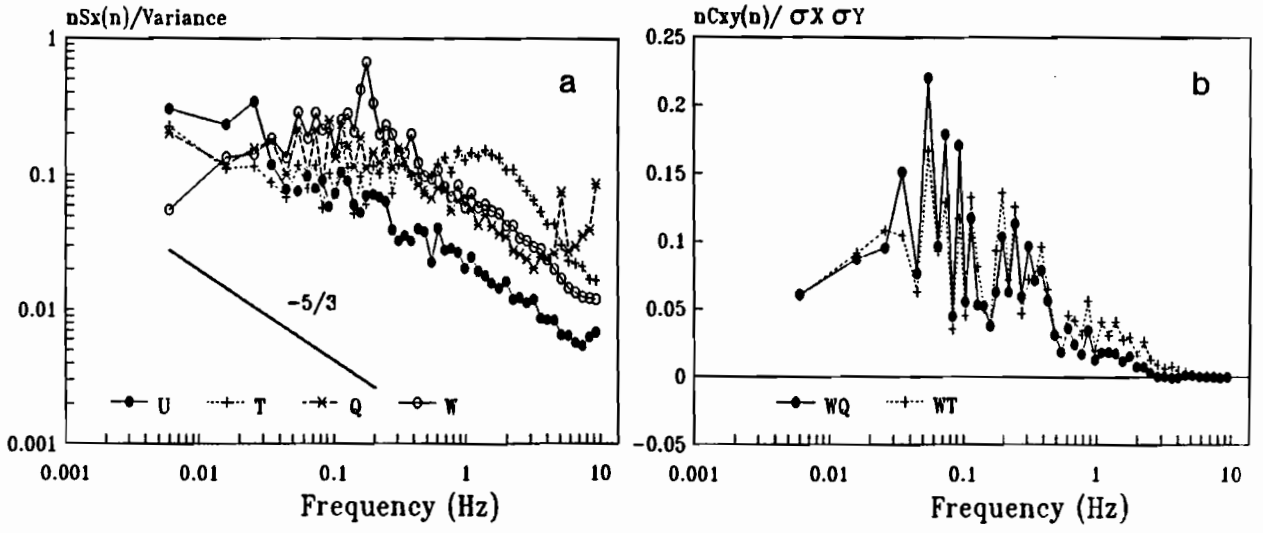

Fig 4. Normalized spectra (a) and Co-spectra (b) for a typical period with low ship motion.

4. RESULTS

4.1 Temperature, humidity and wind measurements

The behaviour of these parameters is illustrated by time sequences during the third observation period, 19–20 May. Figure 5a shows temperatures measured by the psychrometers, the Barton radiometer and the ship's thermosalinograph. There are several notable features. The temperature gradient in the air between 3 and 10 m is extremely small and consistent at 0.2–0.3°C. The difference between these air temperatures and sea temperature at about 2 m below the surface (the 'bulk' temperature) is considerably larger – typically 1–2°C during fine conditions. The sharp decrease in air temperature at 0800 was the outflow from a nearby rainstorm. During the cruise it was not uncommon for the air temperature to fall to as low as 26°C during such storms and the air–sea difference to remain between 2° and 3°C for several hours. These observations are compatible with those from moored buoys in the western equatorial Pacific (McPhaden and Hayes, Lindstrom, personal communication) but at variance with the long-term mean temperature differences obtained from marine climatic data by Esbensen and Kushnir (1981) or by Weare et al. (1981), which are only about 0.5°C in this region.

To examine this further, we have compared four days of air temperature measurements from "Franklin's" routine 2-hourly meteorological observations with those from the 10 m psychrometer on the boom. Agreement was 0.1°±0.6°C for the dry bulb and 0.1°±0.4°C for the wet bulb with the ship's measurement higher in each case. During this period $(T_s - T_a)$, with thermosalinograph temperatures for T_s and the ship's observations for T_a, averaged 1.35°C. So the discepancy remains unexplained. The implications of such large systematic errors for climatological estimates of latent and sensible heat fluxes are discussed below.

The Barton infrared radiometer measures the surface skin temperature of the sea, which is more directly related to the thermodynamic processes which determine sea–air energy exchange rates than is the bulk temperature. With moderate winds and a well-mixed surface layer the difference may well be insignificant; under the conditions we encountered, the skin temperature was typically 0.5°C lower than the thermosalinograph reading and, as in the example shown, can be as much as 0.9°C when the wind speed (Figure 5b) drops completely just before dawn. The surface steadily warmed by 1.5°C through the morning; the thermosalinograph remained steady until 1000 when heating suddenly appeared at this depth. Simple calculation, using reasonable extinction coefficients for the fairly clear water, indicates that sufficient energy penetrates 2–3 m to support the rate of temperature rise shown. The way in which the temperature signal follows the radiation (Figure 5d) and the persistence of the skin temperature depression suggests very little convective mixing in the surface layer. Wind stress is very small until the arrival of a storm at 1600.

The 'cool skin' effect is a possible source of error in the calculation of sensible and latent heat fluxes using bulk transfer equations (2) and (3). Figure 5c shows that use of the infrared temperature to determine vapour pressure at the ocean surface (the saturation value with a 0.98 salinity correction) gives values up to 2 mb lower than those obtained by using the thermosalinograph temperature. The effect of using the bulk temperature is to overestimate both fluxes, partially counteracting the apparent systematic *underestimation* of sea–air temperature difference noted above. Figure 5c also shows vapour pressure at the three boom levels. Some difficulty was experienced with drying out of the psychrometer wet bulbs, and data from the 6 m instrument is missing for most of this day (also, instrument positions were interchanged from time to time; in this case at about 1400). It is clear that the humidity gradient between 3 and 10 m in the air, usually less than 0.5 mb, is very small compared with the air–sea difference of 10–12 mb.

Such small temperature and humidity gradients are extremely demanding of instrumental technique, and effectively rule out the prospect of accurate flux determination using profile methods. Similarly, the wind speed gradients over the 3–10 m height interval were so small as to be almost unmeasurable.

4.2 Latent and sensible heat fluxes and bulk transfer coefficients

Figure 6 shows the eddy-correlation measurements of sensible and latent heat fluxes during the third observation day. Both follow the wind speed (Figure 5b) quite closely as it varied around 1 m/s for most of the day and increased to 4 m/s in late afternoon. Sensible heat flux is small, but always positive, while latent heat flux is an order of magnitude greater.

Altogether 64 h of flux data were recorded during the three observation days. It has been combined with the corresponding measurements of air–sea temperature and humidity difference to calculate bulk transfer coefficients from equations (2) and (3). For most of the time, the sea surface temperatures measured by the infrared radiometer have been used; otherwise those measured by the thermosalinograph. The 6 m psychrometer measurements have been used although, as we have seen, height of measurement in the air is not critical. Total wind speed is the sonic anemometer measurement corrected for the ship speed.

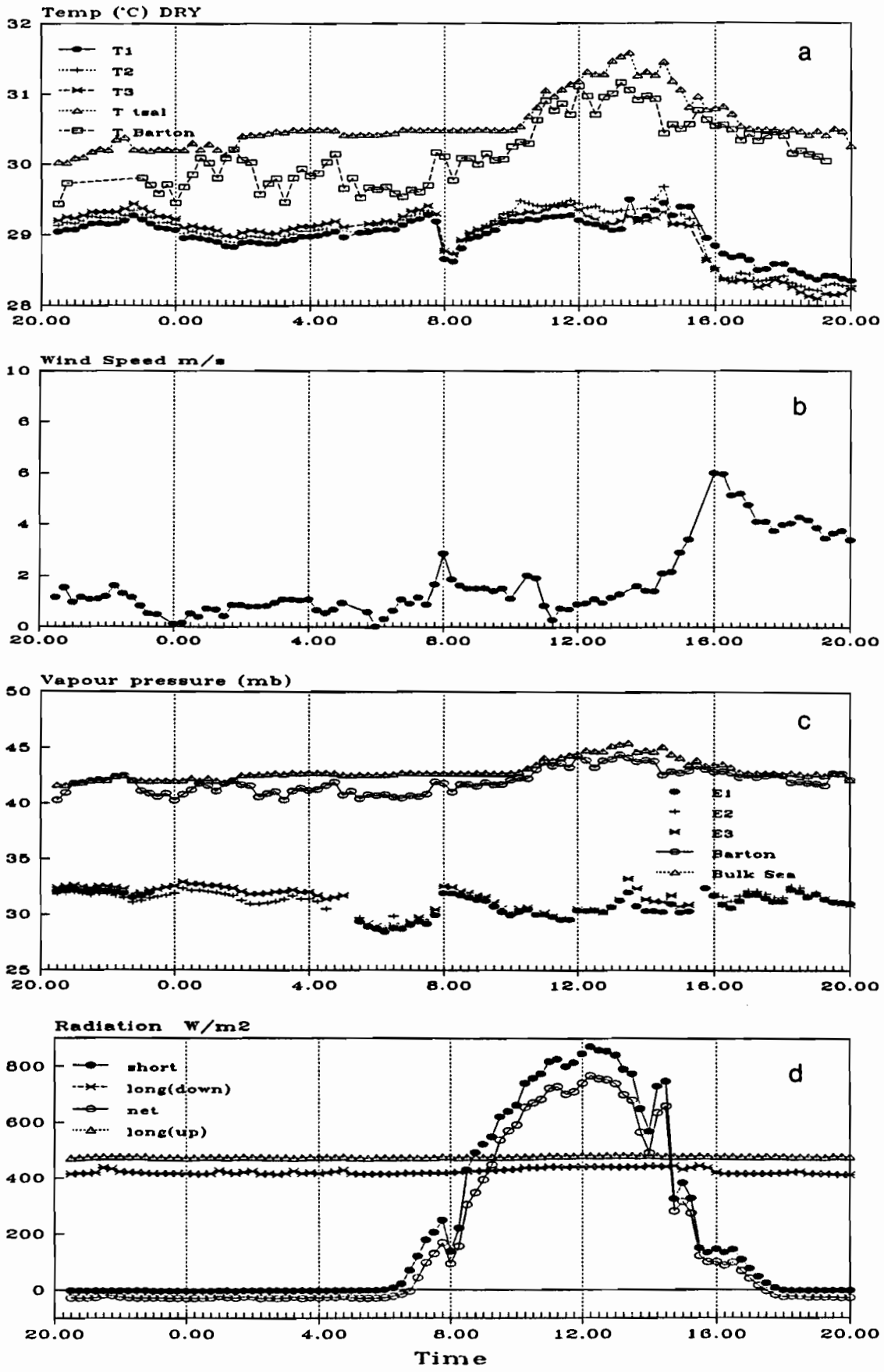

Figure 5. Time sequences of various quantities during third observation period 19–20 May.

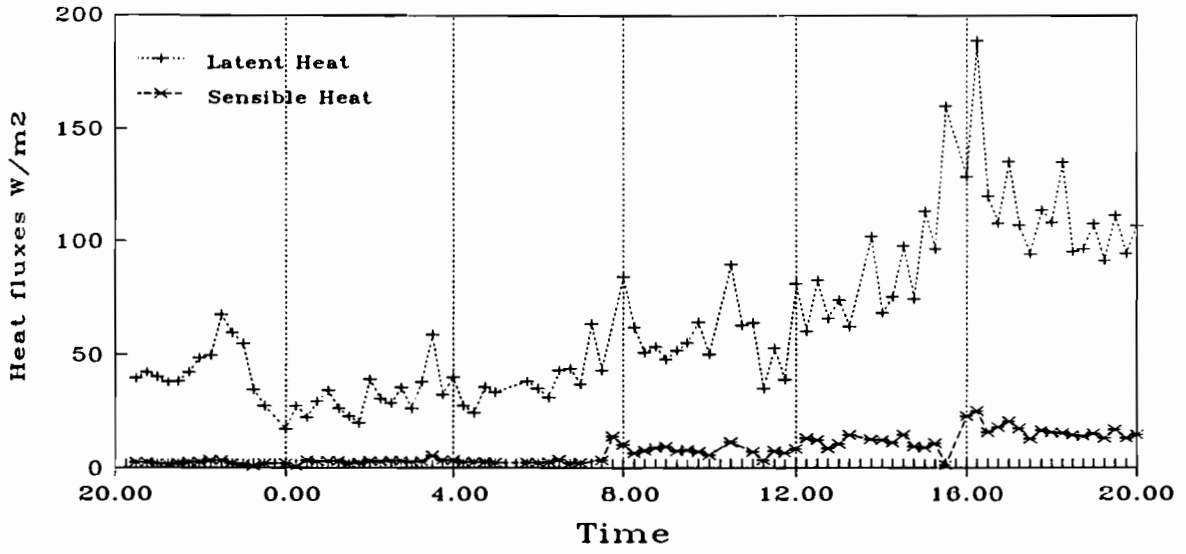

Figure 6. Eddy-correlation measurements of latent and sensible heat during the third observation period 19-20 May.

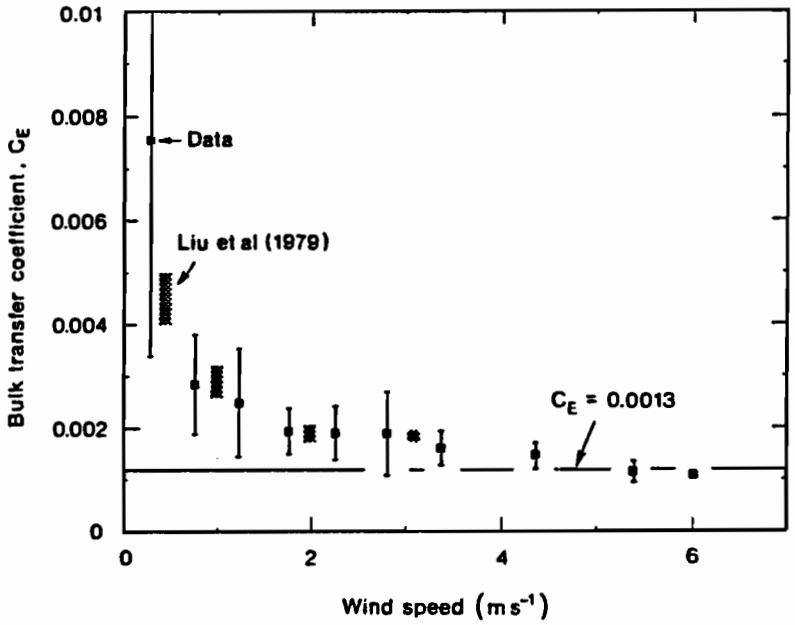

Figure 7. Measured and predicted bulk transfer coefficients for latent heat-flux.

Figure 7 shows the resulting transfer coefficient for water vapour as a function of wind speed. For clarity 15-min measurements have been grouped into 0.5 or 1 m/s wind speed classes and plotted as the mean and standard deviation for each class. The dashed, straight line represents the commonly used value of 0.0013 (e.g. Reed 1985). (A comparison between ten schemes for the parameterisation of C_E is illustrated in Figure 3 of Blanc (1985) and, for these modest wind speeds, C_E ranges from 0.001 to 0.0016.) The hatched areas in Figure 7 give the range of values of bulk transfer coefficients obtained by Liu et al. (1979) for the observed range of sea and air temperatures; their model of the coefficients considers the nature of molecular and sublayer dynamics on either side of the air-sea interface. They predict the rise at low wind speeds, in excellent agreement with the observations. The bulk transfer coefficients for sensible heat are not illustrated here, but behave in a precisely similar fashion. Clearly, in a region where low wind speeds predominate, climate predictions based on conventional transfer coefficients may be significantly in error, as discussed below.

4.3 Dissipation calculations

The inertial dissipation method is being increasingly used to estimate the turbulent fluxes from ships at sea. It is based on the assumption that the spectra of horizontal velocity, $S_u(f)$ and scalars, e.g. $S_q(f)$, (where f is the measured frequency), can be related to the turbulent fluxes of momentum and water vapour through the dissipation rates of turbulent kinetic energy and scalar variance (e.g. Fairall and Larsen 1986). The measurements need only be well behaved, e.g. free from ship motion contamination, in the inertial subrange where the spectra follow the $f^{-5/3}$ relationship. Although much work has been done using this technique, it remains to be shown that the method is applicable under the very unstable, light wind conditions encountered on this cruise. We have calculated the fluxes of momentum and humidity from the relations

$$u_* = [4\alpha_u S_u(f) f^{5/3}]^{1/2} [2\pi/\bar{U}]^{4/3} [kz]^{1/3} [\phi_\epsilon(\xi)]^{-1/3} \tag{4}$$

$$E = \rho L_E [2\pi k z/\bar{U}]^{2/3} f^{5/3} [S_u(f) S_q(f)] [\alpha_u \alpha_q \phi_q(\xi) \phi_\epsilon(\xi)^{1/3}]^{1/2} \tag{5}$$

where k is the von Karman constant, $\alpha_u = 0.55$ and $\alpha_q = 0.8$ are the Kolmogorov constants and $\xi = z/\Lambda$, with the Monin-Obukov Length

$$\Lambda = -u_*^3 T/[gk(\overline{w\theta} + 0.61 T \overline{wq})] \tag{6}$$

where T is absolute temperature, g gravitational acceleration and the unstable dimensionless profile functions, ϕ_ϵ and ϕ_q are given by

$$\phi_\epsilon(\xi) = (1 + 0.5|\xi|^{2/3})^{3/2} \qquad \xi < 0 \tag{7a}$$

$$\phi_q(\xi) = (1 - 14\xi)^{-1/2} \qquad \xi < 0 \tag{7b}$$

The frequency chosen for the spectral estimates was 1 Hz and, as can be seen from Figure 3a, this is in the -5/3 region and clear of either the ship motion at lower frequencies or the vibration problems in q at higher frequencies. The stability corrections, ϕ_ϵ and ϕ_q, were calculated by iteration starting with the neutral dissipation estimates, but with measured $\overline{w\theta}$. The contribution to Λ from $\overline{wq}$ was often comparable to that from $\overline{w\theta}$.

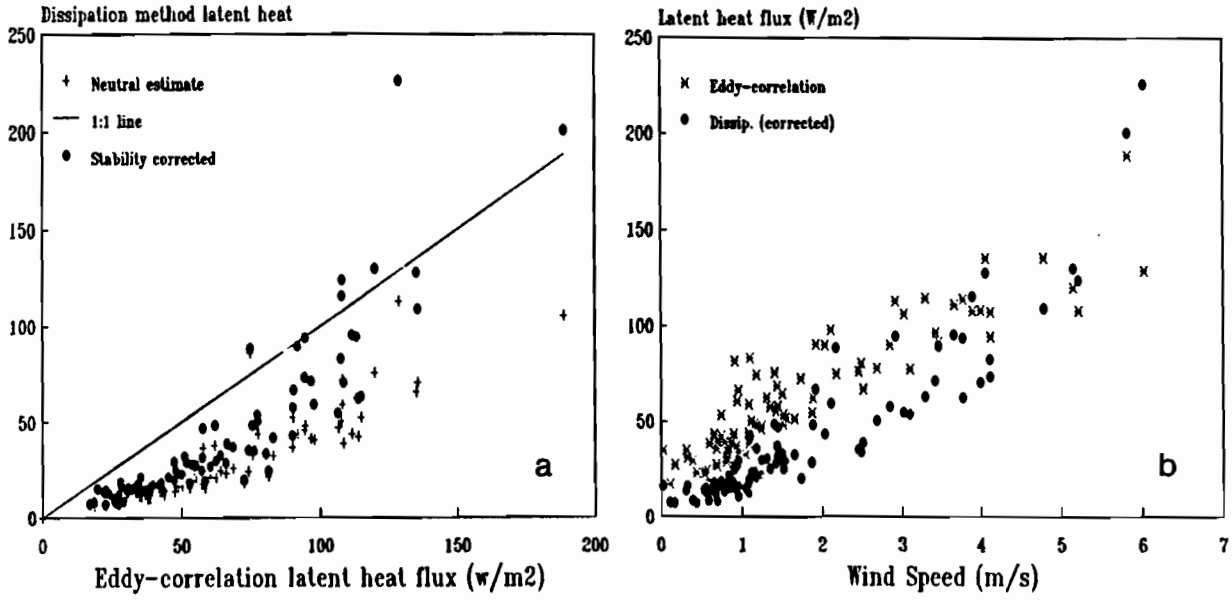

Figure 8. Comparisons of latent heat fluxes derived from eddy-correlation and inertial dissipation methods.

Figure 8a shows the comparison between the covariance and inertial dissipation methods for determining latent heat fluxes. The dissipation method generally underestimates the actual flux but with an improvement

towards higher values of E. In absolute terms the difference is reasonably constant with wind speed (Figure 8b). Some of the assumptions inherent in the inertial dissipation method have questionable validity and the values of some of the constants used have large uncertainty at these low wind speeds and high instabilities (z/Λ approaches −3 and the stability correction approaches a factor of 2): thus the disagreement is not unexpected (Fairall and Larsen 1986, Geernaert et al. 1988).

4.4 Radiation

Radiation measurements through our third observation period appear in Figure 5d. The sky was quite clear during the night, with some light cloud during the day, and became heavily overcast around 1600 with the onset of a storm. Incoming short- and longwave components are directly measured by the pyranometer and pyrgeometer respectively, and outgoing longwave calculated from Stefan's law assuming an emissivity of 0.97 for sea water. The almost constant sea temperature and atmospheric water vapour content lead to a very small diurnal variation in the net longwave balance of 40–60 W/m^2. Assuming an average albedo of 0.08 to account for outgoing shortwave, two estimates of net radiation are available: one from the separate components and the other directly from the net radiometer. A comparison has been made on the basis of 2-hourly averages over the 13-day period 8–20 May, as shown in Figure 9. There appears to be a systematic discrepancy of around 20 W/m^2 in the middle range, which could be explained by poor cosine response of the net radiometer during morning and evening, but overall the agreement is within the accuracy normally accorded such radiation instruments.

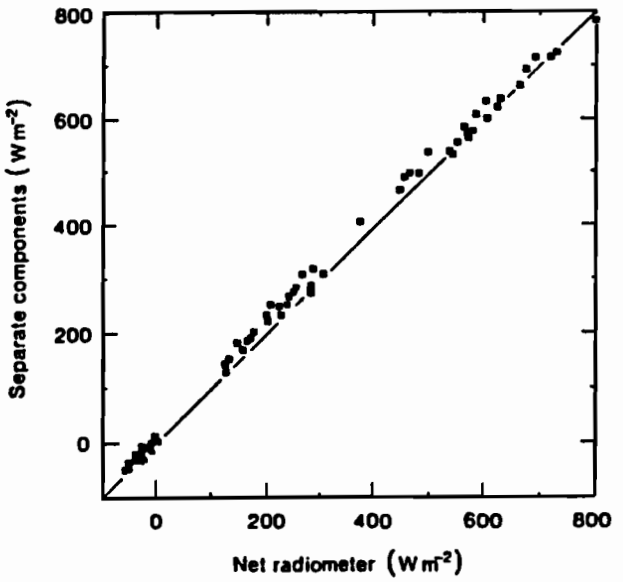

Figure 9. Comparison of net radiation measured in two ways.

5. THE HEAT BUDGET

By analysing ship-of-opportunity meteorological data, Reed (1985) found annual mean values of N into the Pacific near (0°S,150°E) to be between 80 and 100 W/m^2. The results presented above have sufficient resolution (~10 W/m^2) to test the contention by Godfrey and Lindstrom (1989) that long-term heat flux into the region is, in fact, close to zero. Using "Franklin's" routine meteorological observations, we examine the terms on the RHS of Equation (1) over the period 8–20 May. Average daily values of both incoming shortwave and net longwave radiation were very close to the longterm climatology (Esbensen and Kushnir 1981, Reed 1985), indicating that this period, although necessarily short, was sufficiently representative for our purpose. The formulations specified in Reed (1983,Appendix) provide the basis for discussion.

The formula used to predict incoming shortwave radiation is based on solar altitude and mean daily cloud cover. In this region, cloudiness follows a typical diurnal pattern of stormy days and clear nights. Reed (personal communication) accounted for this by including only daytime cloud observations. We have adopted a daytime-weighted modification of the formula which, for the conditions during our 13-day period, reduces the estimate of S by some 25 W/m^2. Our pyranometer measurements for the period average 17 W/m^2 less than the unmodified formula; i.e. the original formula seems to overestimate S, because of the particular cloud conditions by around 20 W/m^2.

The net longwave radiation depends primarily on sea temperature and atmospheric water vapour content as well as cloud cover. Reed's formulation leads to estimates of L which are about **15** W/m^2 less than our measurements (Figure 10), whereas the more complicated version due to Brunt and Berliand (see Budyko 1963) gives much closer agreement.

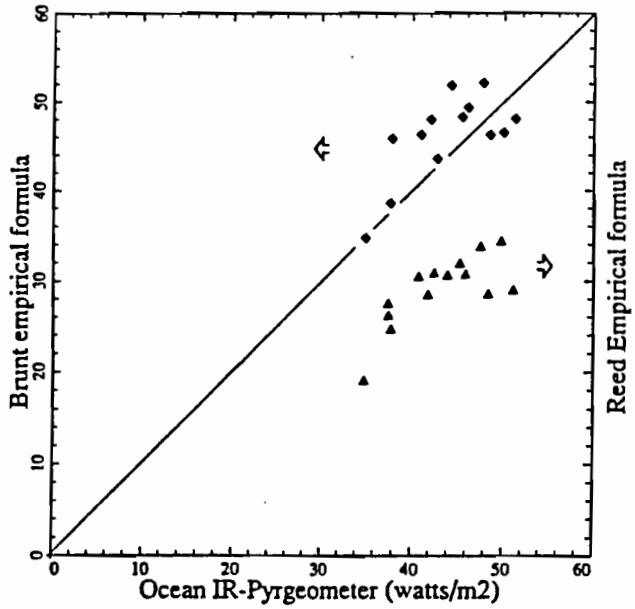

Figure 10. Comparison of two empirical formulae for net longwave radiation, with measurements.

As our measurements show, estimation of sensible and latent heat components of the energy budget using bulk formulae can incur a number of important errors in this particular region. We have shown that the difference ($T_s - T_a$) may be overestimated by perhaps 0.3–0.5°C in the long term due to the 'cool skin', but that there also seems to be a serious discrepancy between merchant ship reports of sea–air temperature difference and our own. Our work suggests that the climatology underestimates sea–air temperature difference by perhaps 0.7–1.0°C, but whether in the measurement of air or sea temperature is difficult to say. If the former, it is probable that the wet bulb and hence q_a are similarly affected; if the latter, the effect ripples through the formulations for q_s, L etc. Sensitivity tests, on the basis of 1°C errors, suggest an overall decrease in N of between **11** and **34** W/m^2.

For the turbulent heat fluxes, it seems more appropriate to use the bulk transfer coefficients of Liu et al. (1979) than the constant value of 0.0013 used by Reed; the difference amounted to **27** W/m^2 for our observation period. The distribution of wind speeds during this time was typical of those in climate atlases, so this value is assumed to represent the longterm effect.

All of the above possible corrections to commonly–used empirical flux formulae operate in the same direction – to reduce estimates of N: in the unlikely event that **all** are valid simultaneously, by between **70** and **100** W/m^2.

Tentative support for small values of net heat flux come from ocean surface layer observations. During May 8–9 "Franklin" deployed a profiling drifter buoy near (4°S,150°E); she returned to the same region on May 20, having followed the track shown in Figure 1. XBT temperature profiles showed that the top 25 m of the sea had warmed by about 0.33°C during the 13 days, which would require a mean heat flux of 30 W/m^2 if it were to be accomplished by local heating. By comparison, our estimates of the net heat flux along "Franklin's" track over the period averaged 38 W/m^2. Such a comparison must obviously be treated with caution; the period was short, the ship travelled into other water bodies and the measurements were interrupted by the port call at Rabaul. However, weather conditions were very consistent day to day over the period, and it seems reasonable to conclude that a substantial fraction of the net heat input of about 40 W/m^2 between May 8 and May 20 was used to heat the surface layer.

6. ACKNOWLEDGEMENTS

None of the above would have been possible without the enthusiastic involvement of Ian Helmond who, among other things, designed the boom. Manuel Nunez and Ian Barton kindly loaned us their radiometers. We are particularly grateful for the support of our cruise leader, Eric Lindstrom, and for the cooperation of Capt. Neil Cheshire and the crew of the "Franklin".

7. REFERENCES

Blanc T.V. (1985) J. Phys. Oceanogr., **15**, 650–669.
Budyko M.I. (1963) Atlas of the Heat Balance of the Earth (in Russian), Kartfabrika Gosgeoltehiyda, 41 pp.
Coppin P.A., and K.J. Taylor (1983) Boundary-layer Meteorol., **27**, 27–42.
Enfield D.B. (1986) J. Phys. Oceanogr., **16**, 1038–1054.
Esbensen S.K., and Y.Kushnir (1981) Climatic Res. Inst. Rep. No. 29, Oregon State University, Corvallis.
Fairall C.W., and S.E. Larsen (1986) Boundary-Layer Meteorol., **34**, 287–301.
Geernaert G.L., K.L. Davidson, S.E. Larsen and T. Mickkelsen (1988) J. Geophys. Research, **93**, 13913–13923.
Godfrey J.S., and E.J. Lindstrom (1989) J. Geophys. Res. (in press)
Hsiung J. (1985) J. Phys. Oceanogr., **15**, 1405–1413.
Legeckis R., W. Pichel and G. Nesterczuk (1983) Boundary-Layer Meteorol., **34**, 287–301.
Lindstrom E., R. Lukas, R. Fine, E. Firing, S. Godfrey, G. Meyers and M. Tsuchiya (1987) Nature, **330**, 533–537.
Liu W.T., K. Katsaros and J.A. Businger (1979) J. Atmos. Sci., **36**, 1722–1735.
Niiler P., and J. Stevenson (1982) J. Mar. Res., **40** Suppl., 465–480.
Ramage C.S. (1984) J. Clim. App. Meteorol., **23**, 187–193.
Reed R.K. (1983) J. Geophys. Res., **88**, 9627–9638.
Reed R.K. (1985) J. Clim. App. Meteorol., **24**, 833–840.
Schlesinger M.E., and J.F.B. Mitchell (1987) Rev. Geophys., **25**, 760–798.
Weare B.C., P.T. Strub and M.D. Samuel (1981) J. Phys. Oceanogr., **11**, 705–717.

CORRIGENDUM

In this paper, some of the radiation estimates are incorrect. Estimates of solar input from Reed's (1983) formula are too small by typically 15 watts/m2, due to use of radians rather than degrees for noon solar angle. In estimating the net outgoing longwave radiation from pyrgeometer readings, the pyrgeometer reading was not multiplied by the emissivity; allowance for this increases the net outgoing longwave radiation by about 13 watts/m2, to 56 watts/m2. Broad conclusions of the paper are not changed. A corrected version will be submitted to J. Geophys. Res.

WESTERN PACIFIC INTERNATIONAL MEETING AND WORKSHOP ON TOGA COARE

Nouméa, New Caledonia
May 24-30, 1989

PROCEEDINGS

edited by

Joël Picaut *
Roger Lukas **
Thierry Delcroix *

* ORSTOM, Nouméa, New Caledonia
** JIMAR, University of Hawaii, U.S.A.

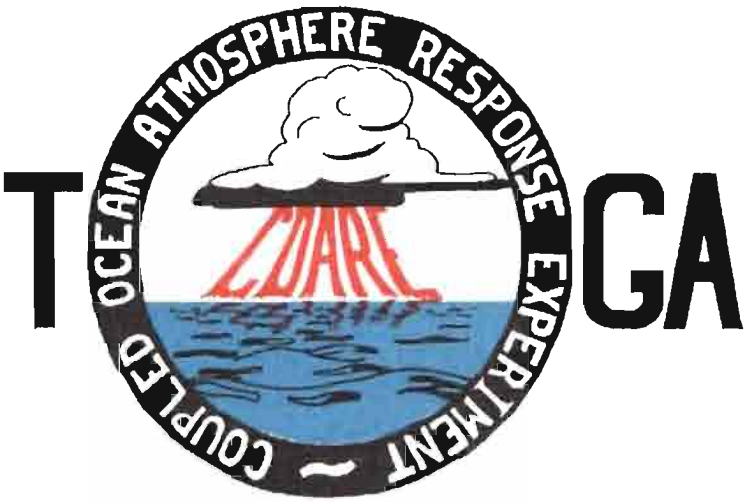

INSTITUT FRANÇAIS DE RECHERCHE SCIENTIFIQUE
POUR LE DÉVELOPPEMENT EN COOPÉRATION

ORSTOM

Centre de Nouméa

TABLE OF CONTENTS

MEETING COLLECTED PAPERS

WATER MASSES, SEA SURFACE TOPOGRAPHY, AND CIRCULATION

EL NINO/SOUTHERN OSCILLATION 1986-87

THEORETICAL AND MODELING STUDIES OF ENSO AND RELATED PROCESSES

MOMENTUM, HEAT, AND MOISTURE FLUXES BETWEEN ATMOSPHERE AND OCEAN

EMPIRICAL STUDIES OF ENSO AND SHORT-TERM CLIMATE VARIABILITY